Water Flow Visualization And Velocity Measurement Using Hydrogen Bubble Generation Technique In Low Speed Open Channel

Asst. Prof. Dr. Akram W. Ezzat **Taif M. Mansoor**
Univ. of Baghdad / Mech. Eng. Dept., Baghdad-Iraq

Abstract

Visualization of water flow around different bluff bodies at different Reynolds number ranging (1505 - 2492) was realized by designing and building a test rig which contains an open channel capable to ensure water velocity range (4-8cm/s) in this channel. Hydrogen bubbles generated from the ionized water using DC power supply are visualized by a light source and photographed by a digital camera. Flow pattern around a circular disk of (3.6cm) diameter and (3mm) thickness, a sphere of (3.8cm) diameter and a cylinder of (3.2cm) diameter and (10cm) length are studied qualitatively. Parameters of the vortex ring generated in the wake region of the disk and the separation angle of water stream lines from the surface of the sphere are plotted versus Reynolds number. Proper empirical formulas are investigated to describe the behavior of vortex ring parameters and separation angle versus Reynolds number. Vortex growth history in the wake region of the cylinder is identified by analyzing the photographs extracted from the digital camera used for photography purposes. Water velocity measurement in the upstream region and near the edge of the disk is conducted at different Reynolds number by measuring the length of Hydrogen bubble pulse streaks generated in the upstream region of the disk using electronic pulse generator circuit. Special electronic circuit is designed and fabricated to cut off the applied DC voltage. The calibration of the designed pulse generator is conducted using the proper oscilloscope device. The pictures extracted from the digital camera are used for analyzing the generated Hydrogen pulses.

Keyword: flow visualization, hydrogen bubble visualization method.

مشاهدة وقياس سرع جريان الماء باستخدام تقنية توليد فقاعات الهيدروجين في قناة مفتوحة ذات سرع واطئة

الخلاصة

تم مشاهدة جريان الماء حول اجسام مختلفة لقيم رينولدز تتراوح (١٥٠٥-٢٤٩٢) من خلال تصميم و تصنيع منظومة تحتوي على قناة مفتوحة تضمن سرع ماء تتراوح (٤-٨سم/ثانية) في هذه القناة. تمت مشاهدة فقاعات الهيدروجين المتولدة من الماء المؤين بواسطة مجهز قدرة للتيار المستمر من خلال اضائتها بمصدر ضوئي وتصويرها عن طريق كاميرا رقمية . تمت الدراسة النوعية لنمط الجريان حول قرص دائري بقطر (٣،٦سم) سمك (٣ملم) و كرة بقطر (٣،٨سم) و اسطوانة بقطر(٣،٢سم)وبطول (١٠سم).

تم رسم علاقة لمحددات حلقة الدوامة المتولدة في المنطقة الخلفية للقرص و زاوية انفصال خطوط جريان الماء من سطح الكرة مع رقم رينولدز. تم ايجاد معادلات تجريبية لتوضيح تصرف هذه المحددات و زاوية الانفصال مع رقم رينولدز. تم تعريف التسلسل الزمني لنمو الدوامة في المنطقة الخلفية للاسطوانة من خلال تحليل الصور من الكاميرا الرقمية المستخدمة لاغراض التصوير. تم اجراء قياس سرعة الماء في المنطقة الامامية و المنطقة القريبة من حافة القرص الدائري عند قيم رينولدز مختلفة من خلال قياس طول شرائح فقاعات الهيدروجين المتولدة بشكل نبضي باستخدام دائرة توليد النبضات الالكتروني. تم تصميم و تصنيع دائرة توليد النبضات الالكترونية لغرض تقطيع الفولتية المجهزة و معايرة هذه الدائرة باستخدام جهاز (اوسكلسكوب) . تم استخدام الصور المستخلصة من الكاميرا الرقمية لغرض تحليل نبضات الهيدروجين المتولدة.

Introduction

Flow visualization is an experimental tool for understanding flow pattern and measuring low fluid velocities. Flow visualization methods could be classified into three groups, addition of foreign material, optical methods and addition of heat and energy. Hydrogen bubble generation technique classified within addition of foreign material group. Hydrogen bubble technique is based on the electrolysis of water. When two electrodes are inserted in the water and a voltage applied between them, hydrogen bubbles are formed at the cathode and oxygen bubbles are formed at the anode. Normally the cathode is a very thin wire of diameter 0.05 mm or less. These wires produce very small hydrogen bubbles in size and the buoyancy forces become negligible compared to hydrodynamic drag forces causing little disturbance of actual flow conditions. A first description of the hydrogen-bubble technique has been given by Clutter and Smith (1961). Shraub et al. (1965) used the Hydrogen bubble technique for quantitative determination of time dependent velocity fields in low speed water flow. Davis and Fox (1967) revised the hydrogen bubble technique and applied it to the measurement of velocity profiles of water flowing in a circular clear plastic tube of the (35 ft x 1 in) dimensions. A tungsten wire of 0.002 in diameter was used as a cathode. Kline et al. (1967) used the hydrogen bubble technique for extensive visual and quantitative studies of turbulent boundary layer. The experiments conducted in open water channels. Water speeds at order of (0.06-0.21 m/sec) were employed. A platinum wire about o.15 m long and 0.025mm diameter was used as a cathode. Burley and Grigg (1970) described a compact solid state unit which provides voltage pulses for the hydrogen bubble flow visualization technique. They used this circuit to visualize boundary layer adjacent to a continuous web of material passing through a liquid. A Nicrom wire of 0.25mm diameter and 3cm length was used as cathode for generating hydrogen bubbles and a brass rod of 3mm diameter was used as anode. Ellis and Stefan (1986) used the hydrogen bubble technique extensively for flow visualization in water and a lesser extent for velocity determination. They used a circuit similar to that used by Shraub et al.[1965]. A tungsten wire of 0.001 in diameter was used as a cathode and hydrogen bubble generator. In this research, the hydrogen bubble velocity meter has proven to be capable of measuring low water velocities (0.4-8 cm/s). Strykowaki and Sreenivasan (1990) used the hydrogen bubble visualization technique to visualize the vortex shedding behind a circular cylinder in a water channel with a free surface at Reynolds number (Re = 80). Hydrogen bubbles generated from 0.05mm diameter steel wires tensioned across the test section orthogonal to the cylinder were used as a flow markers. Mahir and Rockwell (1996) used the hydrogen bubble technique to visualize the wake regions between and downstream of a tandem arrangement of two cylinders. Experiments were carried out in a free surface, closed-loop water channel having a cross-section of (610 mm x 610 mm). The free stream velocity in the channel was (0.03m/s), at Reynolds number (160) based on the cylinder diameter (4.7mm). Platinum wire of diameter 0.025mm was used as a cathode. Hiramoto and Higuchi (2003) used the hydrogen bubble technique to visualize the vortex shedding behind a pair of circular cylinders placed side-by-side at a small angle between them. The experiments were conducted in a water channel with a 0.61 x 0.61m test section. The Reynolds number was 440 based on the free-stream velocity and the diameter of a circular cylinder. The water speed was 0.035 m/s and the diameter of the cylinder was 12.7mm. The angle between the cylinders was 2.2^{o}. Pipe and Monkewtiz (2006) used the hydrogen bubble technique to visualize the vortex shedding from a (3mm) diameter stainless steel cylinder at Reynolds number (50-150). A stainless steel wire with a diameter of (70 μm) held parallel to the cylinder axis was used to perform flow visualization of the cylinder wake. Garica et al. (2007) used the hydrogen bubble technique to visualize qualitatively the flow in tubes of (32mm) diameter with wire coils. The test section had been placed at a distance of 45 diameters from the tube entrance to ensure a fully developed flow condition. A copper wire was used as a cathode for generating hydrogen bubbles.

The objective of present work uses the hydrogen bubble generation technique to study qualitatively and quantitatively the flow patterns around bodies with different shapes in open water channel. Low water velocity range (4–8 cm/sec) is used in the experiments which ensure different Reynolds number around the bluff bodies.

Vortex ring parameters and shear layer geometry in the wake region of a circular disk versus Reynolds number are investigated, flow separation around a sphere and the vortex growth history around cylinder are identified.

Investigation the relationship between the normalized velocities near the edge of the circular disk versus Reynolds number is conducted using quantitative approach of Hydrogen bubble generation.

Experimental Set-Up And Procedure

Fig.1 shows the system used in the present work which is designed and built according to water velocity range inside the water channel. A rectangular cross section glass water channel (1.5m length × 0.12m width × 0.15m depth) dimensions is used for the visualization of the water flow patterns around bluff bodies. The entrance and the exit of open channel is made in conical shape to ensure steady and uniform free stream lines as much as possible.

Downstream of the test section channel a feed tank of (70cm × 15cm × 40cm) dimensions is fixed to provide constant water flow rate into the test section during water velocity measurements. The open channel receives water from the feed tank by (1in) diameter PVC type pipe which is fixed parallel to the channel inlet.

A (SAER) type pump of (0-6m³/h) discharge is used for circulating the water in the test section. A PVC (LZS-32) type flow meter is used for the measurement of water flow rate in the open channel. The range of the flow meter is (0.6-6 m^3/h).The water flow rate in the test section is controlled by two valves. One of these valves is fixed in the water feed line of the test section while the other is fixed in the bypass line between the downstream and upstream lines of the test section.

A (FARNELL L 30E 30volts-5 Amp) type power supply was used for water ionization .The voltage from this power supply was cut off by means of pulse generation circuit. This pulse generation circuit is used for quantitative measurements. A square wave pulse generation circuit shown in Fig.2 is used in the present experiments which was designed and built according to water velocity range inside the test section. It consists of IC 555 timer, two variable resistances (10kΩ, 4MΩ) and two capacities (1μF, 0.01μF). Rv1 was used to change the pulse duration time. Pulse generation circuit is checked and calibrated before usage by a (UT3025C) type digital storage oscilloscope. The electronic circuit that has been constructed in the present experiments to cut off the applied voltage and generate the hydrogen bubbles streaks for quantitative measurements is shown in fig.3. Sony (DSC-S2100) type digital camera is used for photography purposes of the instantaneous generated hydrogen bubbles illuminated by a light source of 1000W tungsten halogen bulb fixed a side of the channel in front of the slit prepared to pass the light in a direction parallel to the level of water ionization wire fixed inside the open channel. The test section consists of a hydrogen bubble Generation wire and photographic setup which is installed at (60cm) distance from water entrance to the test section. In the present experiments, a copper wire of 0.05mm diameter is used as a cathode for generation hydrogen bubbles. The production of acceptable light levels and contrast is strongly dependent on the angle of the incident light on the bubbles with respect to the line of sight of the camera or viewer. For best results this angle should be approximately (65˚) with respect to the perpendicular line drawn on the water surface in the opposite direction of the incident light [Shraub et al. (1965)]. Dark background is necessary and all incidents light other the collimated sheet should be minimized.

Results And Discussion

A- Qualitative Investigation

Fig.4.shows the vortex ring formed behind a circular disk of (3.6cm) diameter at different Reynolds number ranging(1605-2216).Vortex parameters measured directly from the above mentioned figure plotted versus Reynolds number which is based on disk diameter and the water velocity in the upstream region of the disk as shown in figures (5), (6) and (7) .These figures show that vortex ring radius and the distance between the vortex edge and disk edge are proportional to the Reynolds number, as they are increasing by increasing Reynolds number.

Following relationships are investigated for the above proportionalities which are applicable for the above mentioned range of Reynolds number:

$$\frac{r_v}{R_D} = 4.75 \times 10^{-8} (Re)^{2} \quad (1)$$

$$\frac{S_v}{R_D} = 1.38 \times 10^{-5} (Re)^{1.3} \quad (2)$$

Fig.8 shows the shear layer affected zone, shear layer thickness formed behind a circular disk of (3.6cm) diameter at different Reynolds number ranging (1605-2492). Shear layer parameters measured directly from the above mentioned figures are plotted versus Reynolds number based on disk diameter and the water velocity in the upstream region of the disk as shown in figures (9) and (10) which show that the distance between the position of maximum shear layer thickness and the disk rear surface and the distance between the edge of maximum shear layer thickness and the disk edge are proportional to the Reynolds number as they are increasing by increasing Reynolds number.

Following relationships are investigated for the above proportionalities which are applicable for the above mentioned range of Reynolds number:

$$\frac{X_m}{D} = 3.2 \times 10^{-6} (Re)^{1.6} \quad (3)$$

$$\frac{S_m}{D} = 2 \times 10^{-3} (Re)^{0.7} \quad (4)$$

Fig.11 shows the growth history of the vortex behind a (3.2 cm) diameter cylinder at Reynolds number (Re =1623).The justification of this growth history is that boundary layer over the cylinder surface separates due to the adverse pressure gradient imposed by the divergent geometry of the flow environment at the rear side of the cylinder. As a result of this, shear layer is formed. The boundary layer formed along the cylinder contains a significant amount of vorticity. This vorticity is fed into the shear layer to roll up into a vortex with a sign identical to that of the incoming vorticity. Vortex (B) will grow larger than the other (A). The vorticity in the one of these vortices is in the clockwise direction, while the vorticity in the other vortex is in the anti-clock wise direction. Both directions are towards the centerline of the open channel where the wake velocity behind the cylinder approvers to zero.

Fig.12 shows the separation of streamlines from the surface of (3.8cm) diameter sphere at different Reynolds number ranging (1505-2414). Separation angle (θ) versus Reynolds number (Re) are plotted as shown in Fig.13 which shows that separation angle (θ) is proportional to the Reynolds number, (θ) as it increases by increasing Reynolds number.

Following relationships is investigated for the above proportionality which is applicable for the above mentioned range of Reynolds ranging (1500-2500):

$$\theta = 75 + 1.76 \times 10^{-3} Re^{1.1} \quad (5)$$

B- Quantitative Investigation:

Fig.14 shows the hydrogen streak generated in the water flowing in the open channel using the pulse generator circuit at different flow rates ranging (1.6-3.1 m^3/h). The streak length generated from water ionization is proportional to the water velocity by using the following equation:-

$$U\infty^{\circ} = L_h \times CF \times f \quad (6)$$

Fig.15 shows the water velocity measurement using the hydrogen bubble generation ($U\infty^{\circ}$) versus its magnitude using water flow meter ($U\infty^{*}$). Fig.16 shows the hydrogen streak generated near the edge of the disk using the pulse generator circuit at different Reynolds number ranging (1533-1680). The streak length generated from water ionization is proportional to water velocity.

Fig.17 shows that the absolute U_e° values of the water velocity near the edge of the disk measured using hydrogen bubble generation technique increases by increasing the velocity in the upstream region of the disk, $U\infty^{\circ}$, knowing that the effect of the channel walls on water velocity is excluded by replacing the absolute values of the water velocity near the edge of the disk U_e°, by corrected value ($U\infty_c^{\circ}$) according to the real flow area:-

$$U\infty^{\circ}_c = \frac{U\infty^{\circ} \times A}{A - A_d} \quad (7)$$

Fig.18 shows the normalized value of water velocity near the edge of the disk to its value in the upstream region of the disk ($U_e^{\circ}/U\infty^{\circ}$) versus Reynolds number. It is clear that the average value of this ratio is (1.08).

Conclusion

1-Radial and axial distance of the vortex formed in the wake region of a disk in low range of water velocity and its radius are proportional to the Reynolds number based on disk diameter, this could be concluded from equations(1) and (2).

2- The boundary of the wake region prolongs axially and radically to further distances as Reynolds number increases as shown from the figures related to the wake region of circular disk. This could be concluded from equations (3) and (4).

3- The separation of streamlines from the surface of the sphere proves that separation in the laminar range of Reynolds number which is ranging from (1505-2414) takes an average value of (82.5°).

4- The pictures related to the wake region of cylinder prove that the shear layer formed along it contains a significant amount of vorticity and that the formations of these vortices are random. This conclusion is proved by some pictures extracted from the wake region of the cylinder at different time intervals

The quantitative approach of the study concludes the following:

1- The average normalized value of water velocity near the edge of the disk to its value in the upstream of the disk using hydrogen bubble generation technique demonstrates that water velocity near the edge of the disk increases by (8%). This estimation excludes the effect of water flow area change between the disk edge and the channel wall.

2-The reliability of water velocity measurement using hydrogen bubble generation is limited to velocity rang lower than 8 cm/sec with percentage error of 5% due to the adverse effect of flow disturbance on the bubbles during its movement with water flow which prevent the visualization when these bubbles across the light slit to higher lever.

Reference

Burley, R., and Grigg, P.J., "**A Solid State Pulser for the Hydrogen Bubble Flow VisualizationTechnique**" J.Phys.E:Sci.Instrum, Vol.3, 1970, PP.1018-1020.

Clutter, D.W. and Smith, A.M.O., "**Flow Visualization by Electrolysis of Water"**, Aerospace Eng, Vol. 20, 1961, pp. 24-27.

Davis, W., and Fox, R.W., "**An Evaluation of the Hydrogen Bubble Technique for the Quantitative Determination of Fluid Velocities within Clear Tubes**", Journal of Basic Engineering, Vol. 89, 1967, PP. 771-781.

Ellis, C.R. and Stefan, H.G., "**Development of Hydrogen Bubble Velocity Meter** ", Journal of Hydraulic Engineering, Vol.112, 1986, pp. 59-64.

Garcia, A. Solano, J.P., Vicente, P.G., and Viedma, A., "**Flow Pattern Assessment in Tubes with Wire Coil Inserts in Laminar and Transition regimes** ", International Journal of Heat and Fluid Flow, Vol. 28, 2007, PP. 516-525.

Hiramoto R. and Higuchi H., "**Vortex Shedding behind a Non Parallel pair of Circular Cylinders** "Journal of Fluids and Structures, Vol. 18, 2003, PP. 131-143.

Kline, S. J., Reynolds W.C., Shraub F.A. and Runstadler P.W., "**The Structure of Turbulent Boundary Layer"**, Journal of Fluid Mechanics, Vol. 30, 1967, pp. 741.

Mahir, N., and Rokwell, D. ,"**Vortex Formation from a Forced System of Two Tandem Arrangement Cylinders** ", Journal of Fluids and Structures, Vol.10, 1996, PP.473-489.

Pipe, C.J. and Monkewtiz, P.A., "**Vortex Shedding in Flows of Dilute polymer solutions**", Journal of Non-Newtonian Fluid Mechanics, Vol. 139, 2006, pp. 54-67.

Shraub, F.A., Kline, S.J., Henry, J., Runstadler, P.W., and Littell , JR. A. "**Use of Hydrogen Bubbles for Quantitative Determination of Time-Dependent Velocity Fields in Low-Speed Water Flows**", Journal of Basic Engineering, Vol. 87, 1965, PP. 429-444.

Strykowski, P.J., and Sreenivasan, K.R., "**on the Formation and Suppression of Vortex Shedding at Low Reynolds Numbers** ", Journal of Mechanics, Vol. 218, 1990, PP.71-107.

Nomenclature

Symbol	Meaning	Units
A	Flow cross section area	cm^2
A_d	Disk area	cm^2
CF	Correction factor based on the ratio of the real disk diameter to the disk diameter as measured from the photo	
D	Diameter of the disk	cm
f	Pulse frequency of pulse generator	s^{-1}
L_h	The length of the hydrogen bubbles line as measured from the photographs	cm
Q	Water flow rate	m^3/h
Re	Reynolds number	
R_D	Radius of the disk	cm
r_v	Radius of the vortex ring	cm
R_v	Distance between the vortex ring center and the disk center	cm
S	Shear layer thickness, the distance between the outer edge of the disk and the edge of shear layer initiated in the wake region of the flow across disk.	cm
S_v	Distance between the outer edge of vortex ring and the outer edge of the disk	cm
S_m	The distance between the edge of maximum shear layer thickness and the disk edge	cm
t	Time	Sec
$U\infty^{o}$	Upstream water velocity measured by hydrogen bubble technique	cm/sec
$U\infty^{*}$	Upstream water velocity measured by flow meter	
U_e^{o}	Velocity at the edge of the disk measured by hydrogen bubble technique	cm/sec
X_m	The axial distance between the position of maximum shear layer thickness and the disk rear surface	cm

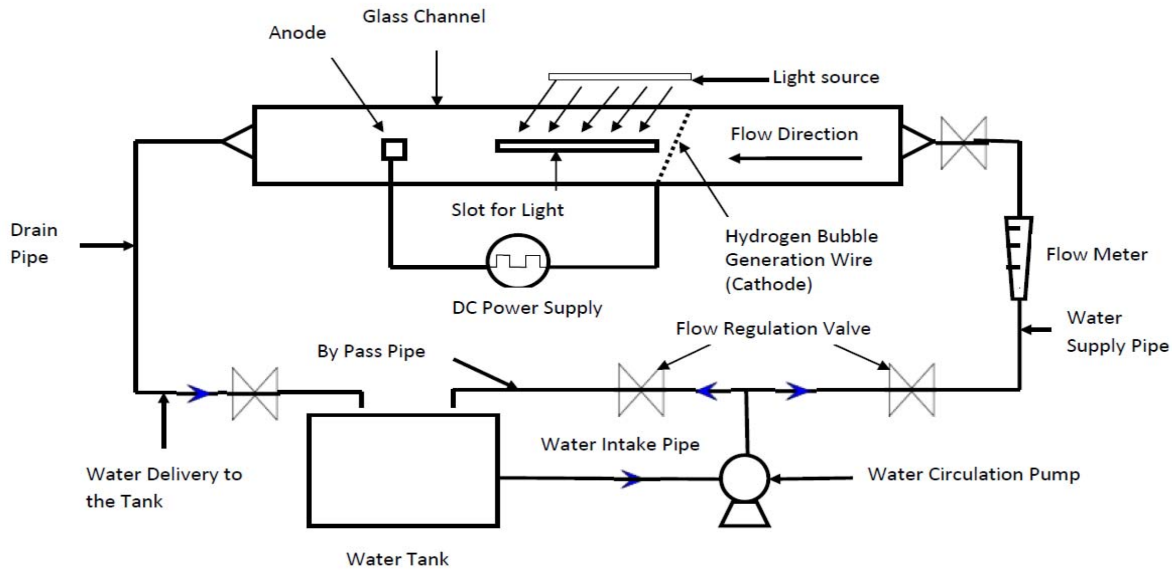

Fig.1. Configuration of water velocity measurement and flow visualization system using hydrogen bubble generation technique

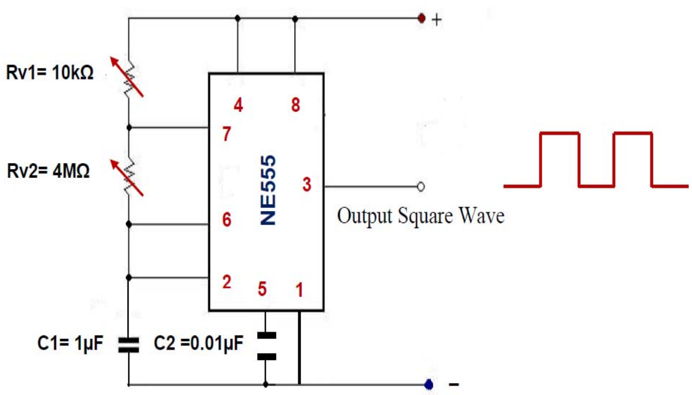

Fig. 2. Simple electronic voltage pulsing circuit with IC555 timer used in the present experiments.

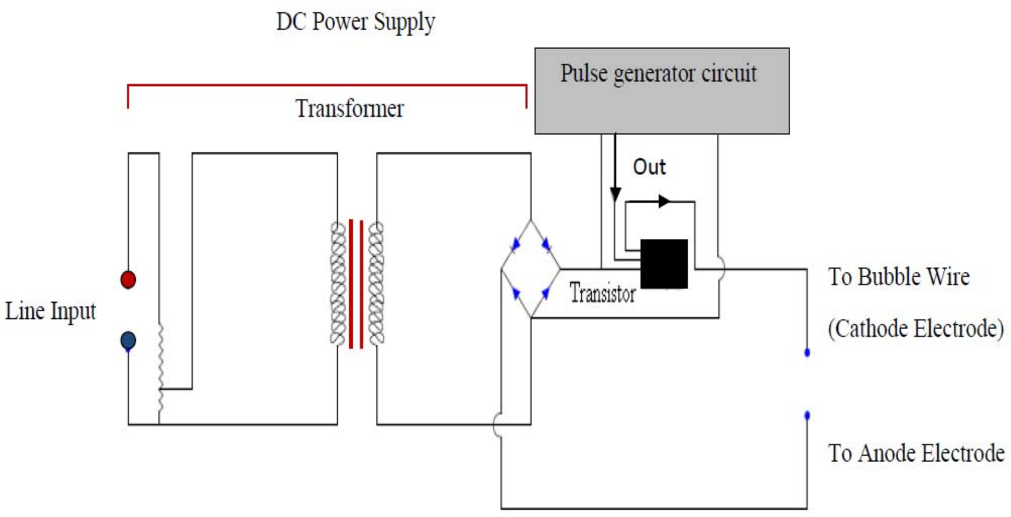

Fig.3 The electronic circuit used in the present experiments.

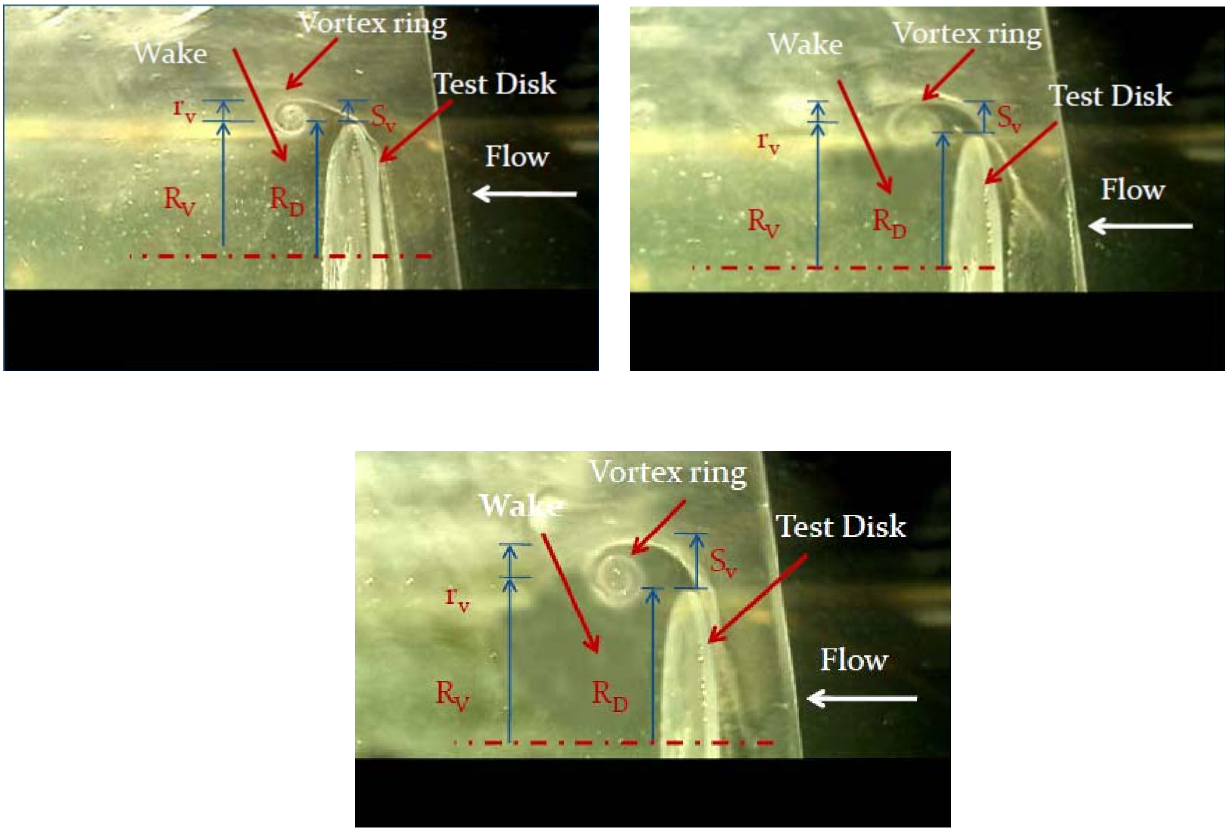

Fig.4. Vortex ring formed behind a (3.6cm) disk at Reynolds number: A (Re= 1605), B (R= 1887), C (Re= 2216)

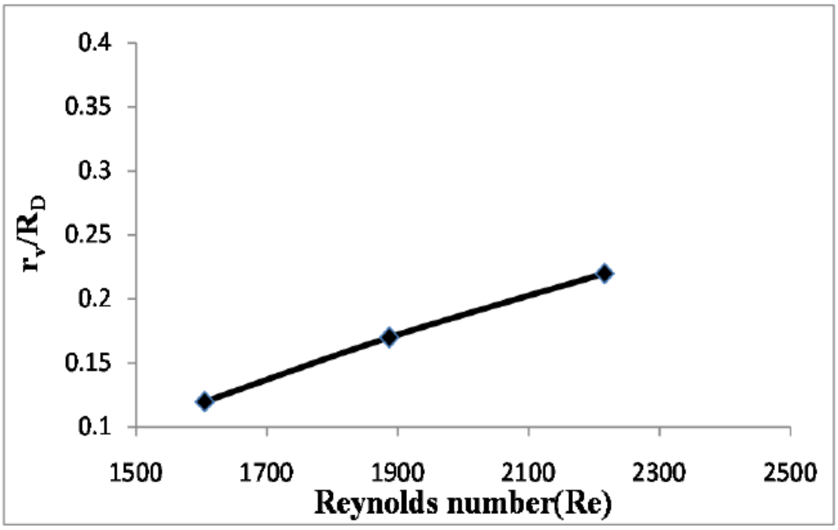

Fig.5. Normalized vortex ring radius to the disk radius versus Reynolds number.

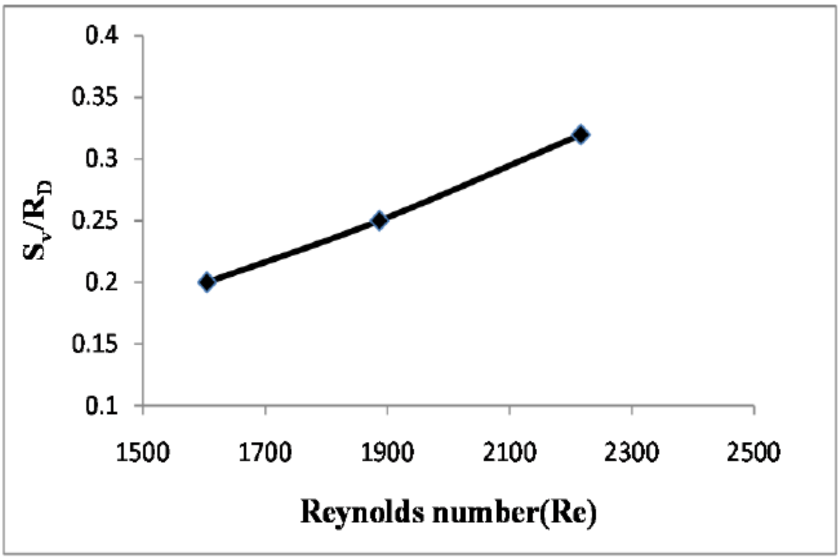

Fig.6. Normalized distance between vortex ring edge and disk edge to the disk radius versus Reynolds number

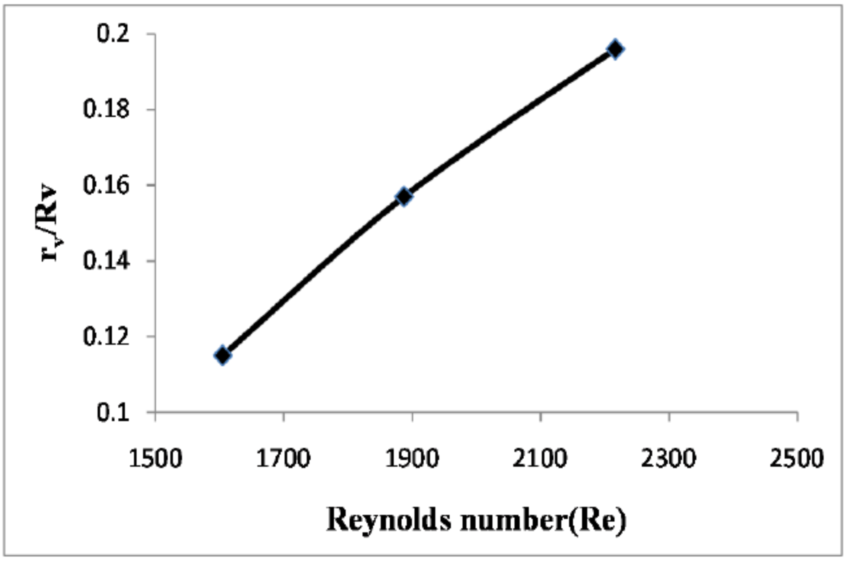

Fig.7. Normalized vortex ring radius to the distance between vortex ring center and disk center versus Reynolds number

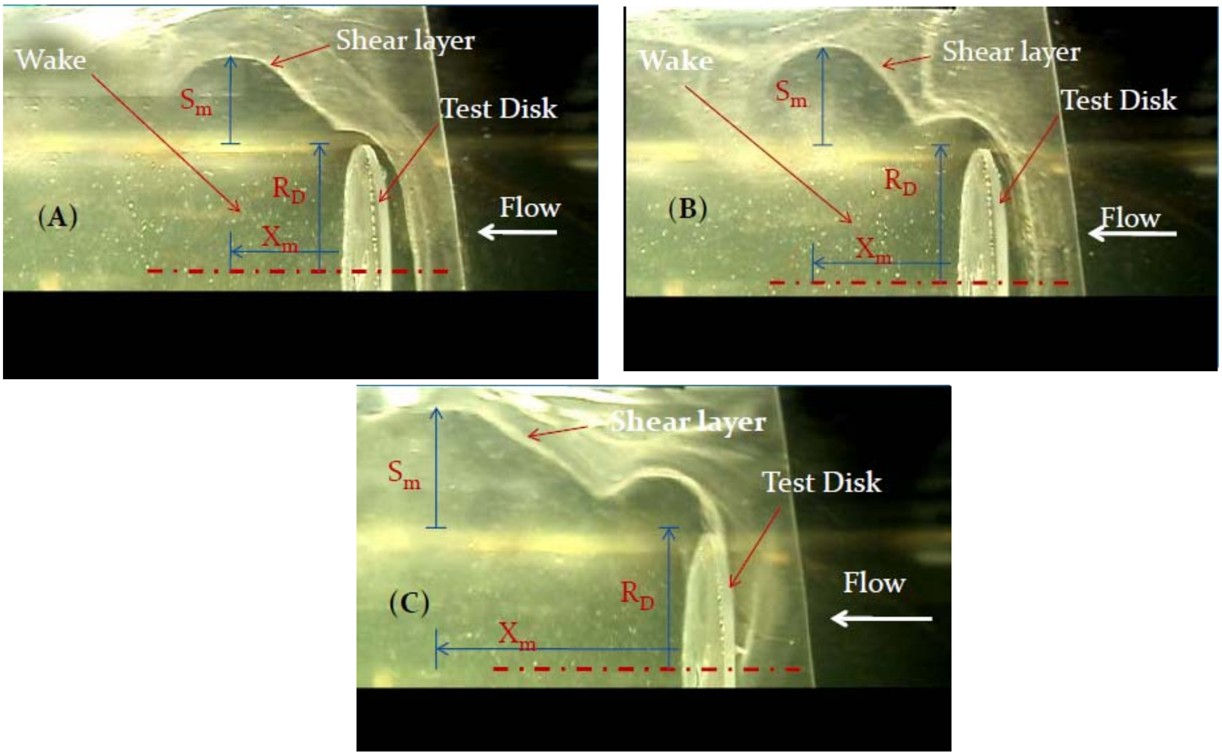

Fig.8. The wake boundary, shear layer affected zone behind a (3.6) cm disk at Reynolds number A (Re= 1605), B (R= 1887), C (Re= 2216)

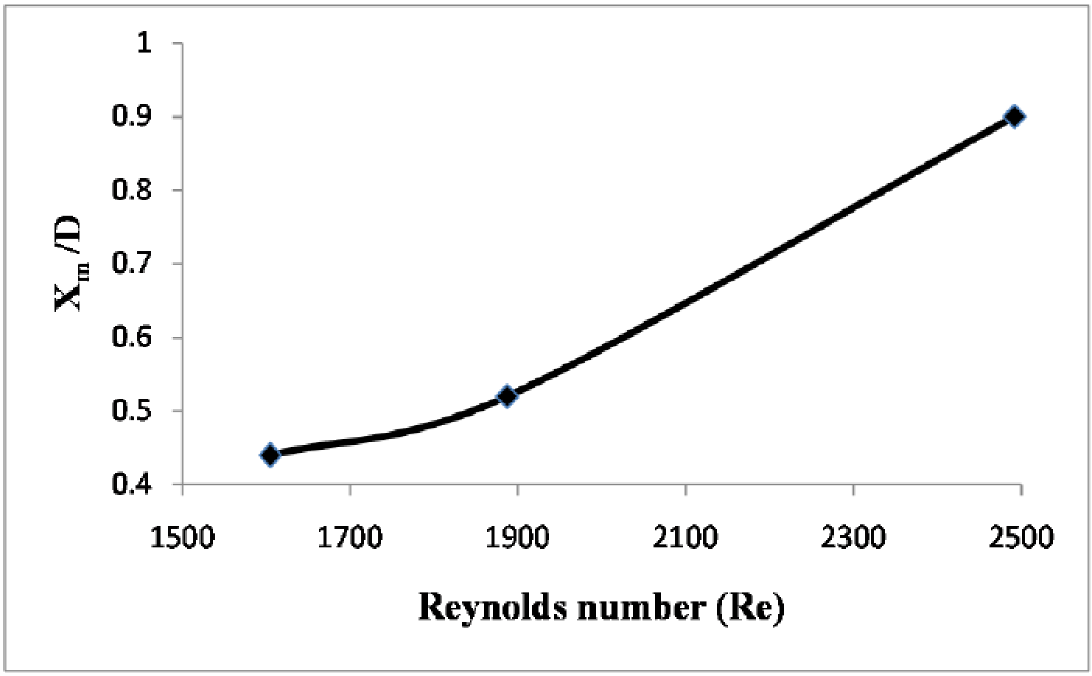

Fig.9. Normalized distance between the position of maximum shear layer thickness and disk rear surface to the disk diameter versus Reynolds number

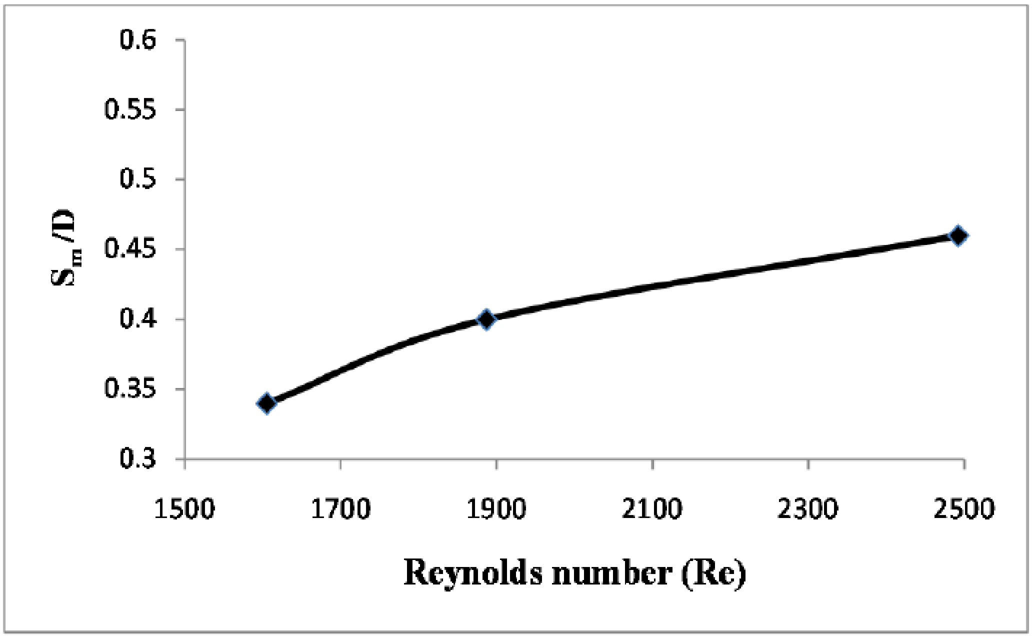

Fig.10. Normalized distance between the edge of maximum shear layer thickness and the disk edge to the disk diameter versus Reynolds number.

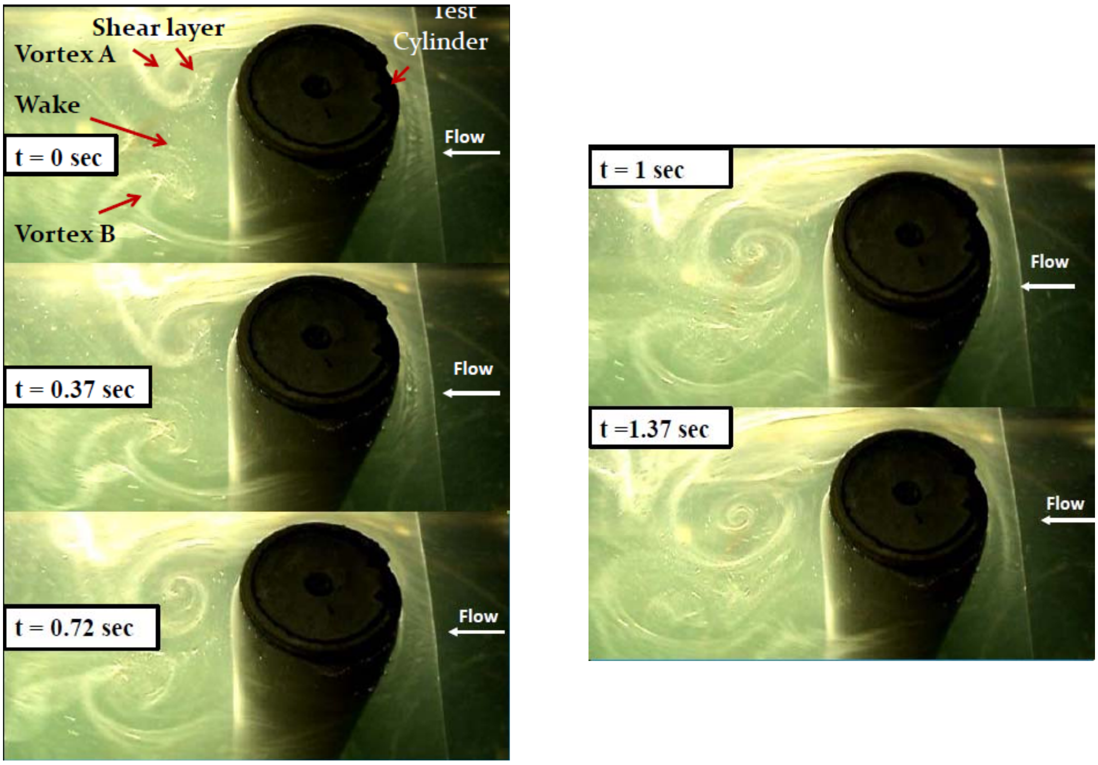

Fig.11. Development of vortex shedding in the wake region of (3.2cm) diameter cylinder at (Re =1623) during different elapsed time intervals

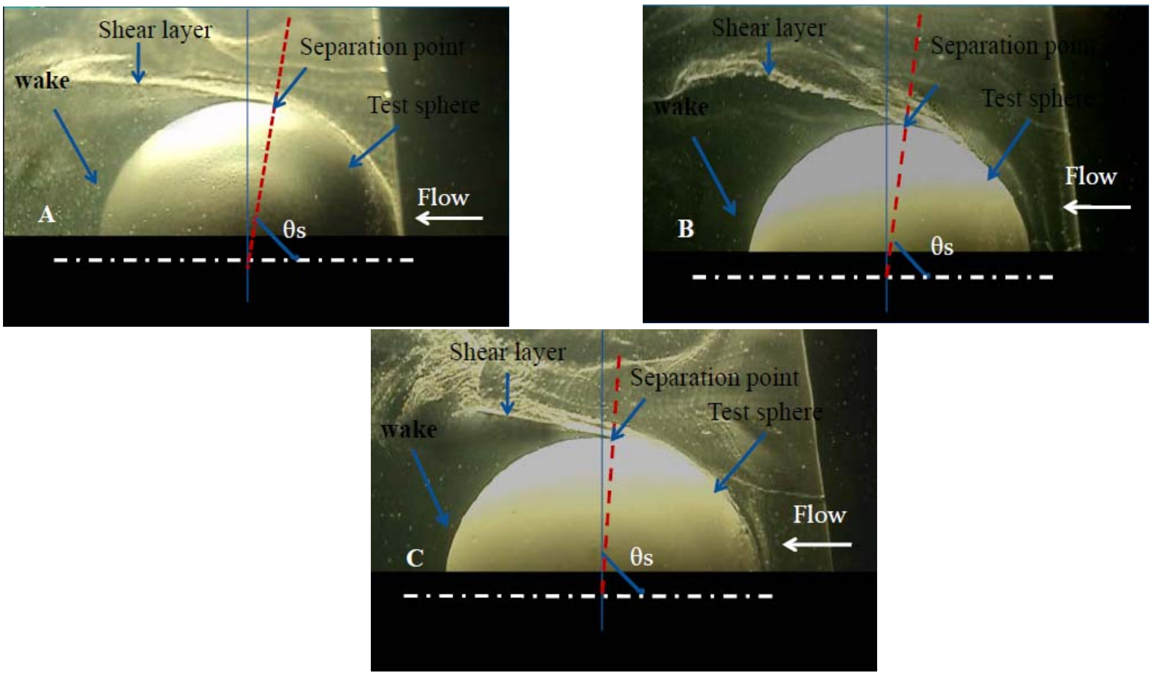

Fig.12. Flow separation from (3.8cm) sphere surface at Reynolds number A (Re= 1605), B (R= 1887), C (Re= 2216)

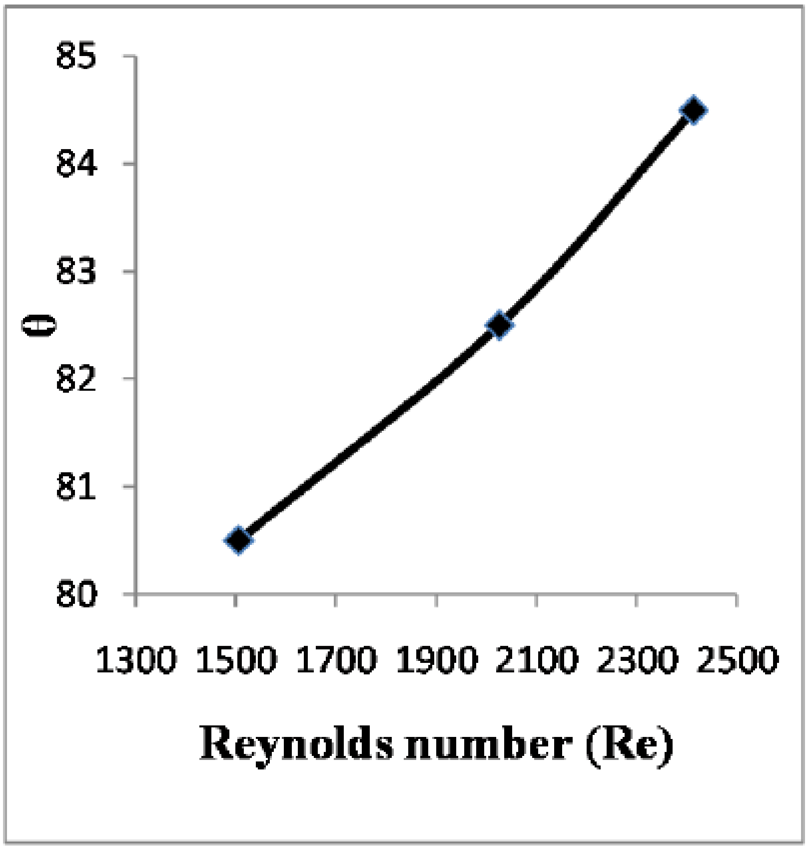

Fig.13 Flow separation angle from a (3.8cm) sphere surface versus Reynolds number

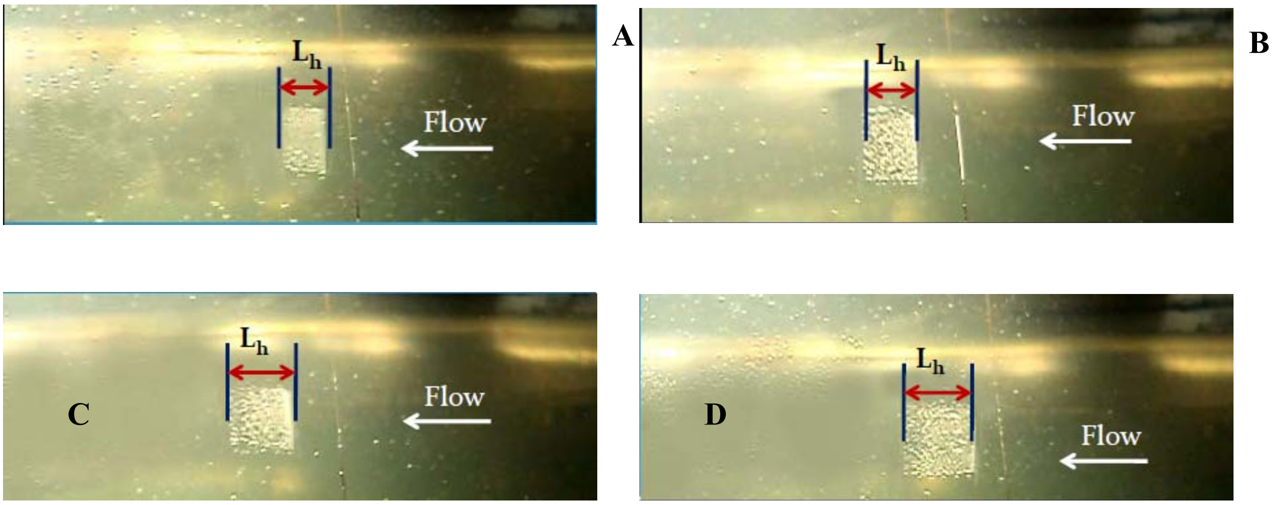

Fig.14. Water average velocity measurement in the open channel using hydrogen bubble generation technique at water flow rates: A (Q=1.6 m^3/h), B (Q= 2.1 m^3/h), C (Q=2.7 m^3/h), D (Q =3.1 m^3/h)

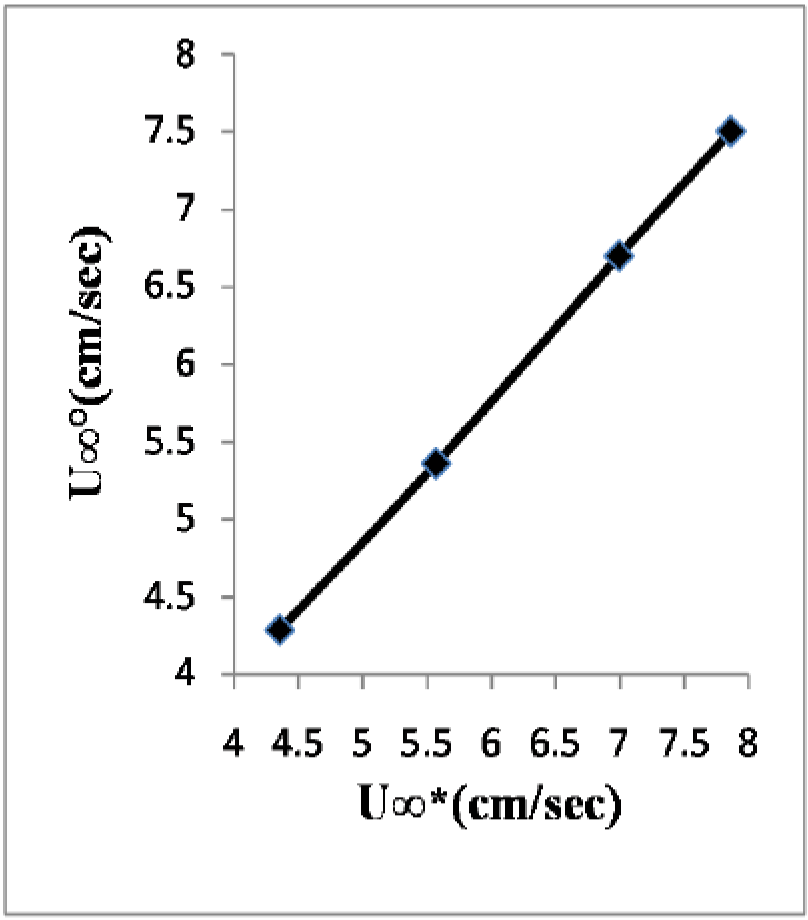

Fig.15. Water velocity measured using hydrogen bubble generation, U∞° versus its magnitude based on the water flow rate measurement, $U\infty^*$ in the open channel

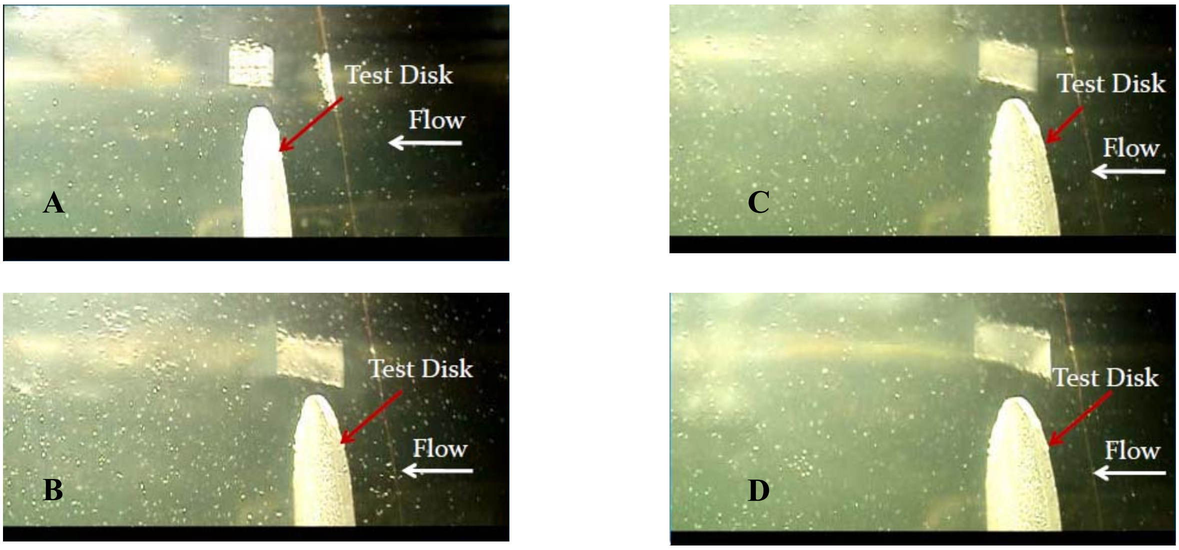

Fig.16. Water velocity measurement near the edge of the disk at Reynolds number: A (Re= 1533), B (R= 1916), C (Re= 2395), D (Re= 2680)

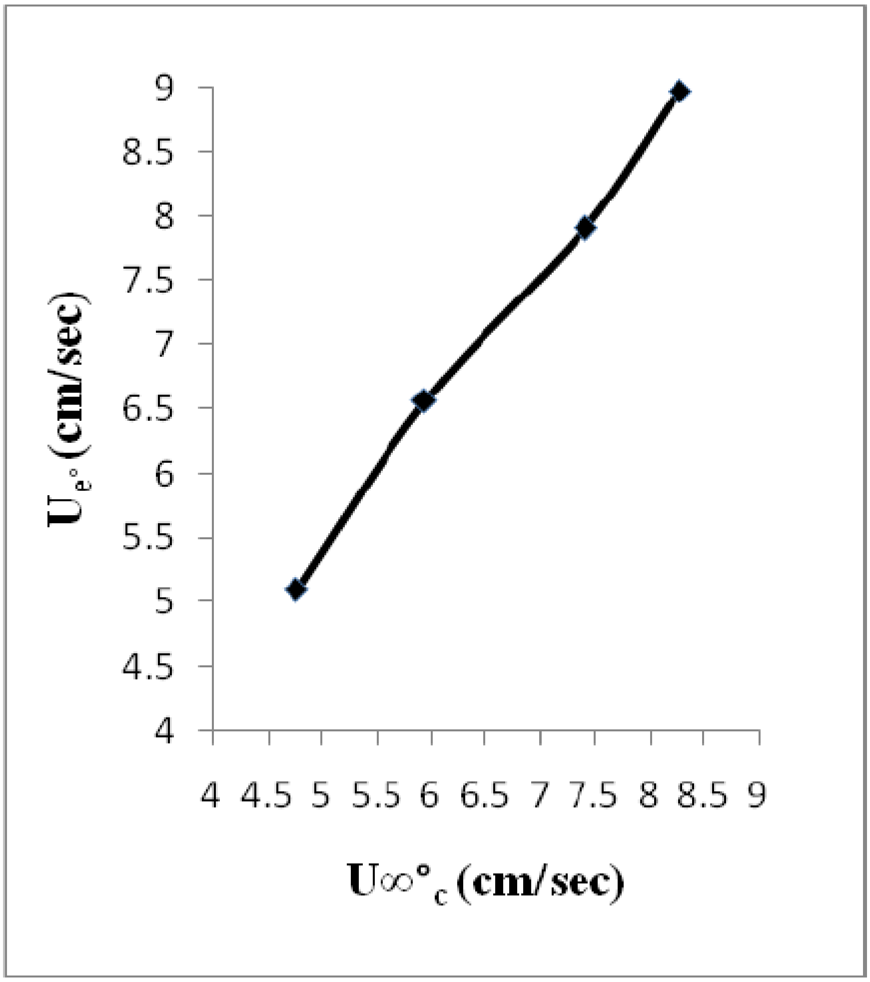

Fig. 17: Water velocity near the edge of the disk, U_e° versus its value in the upstream of the disk corrected according to the new flow area, $U_{\infty}^{\circ}{}_c$ using hydrogen bubble generation technique.

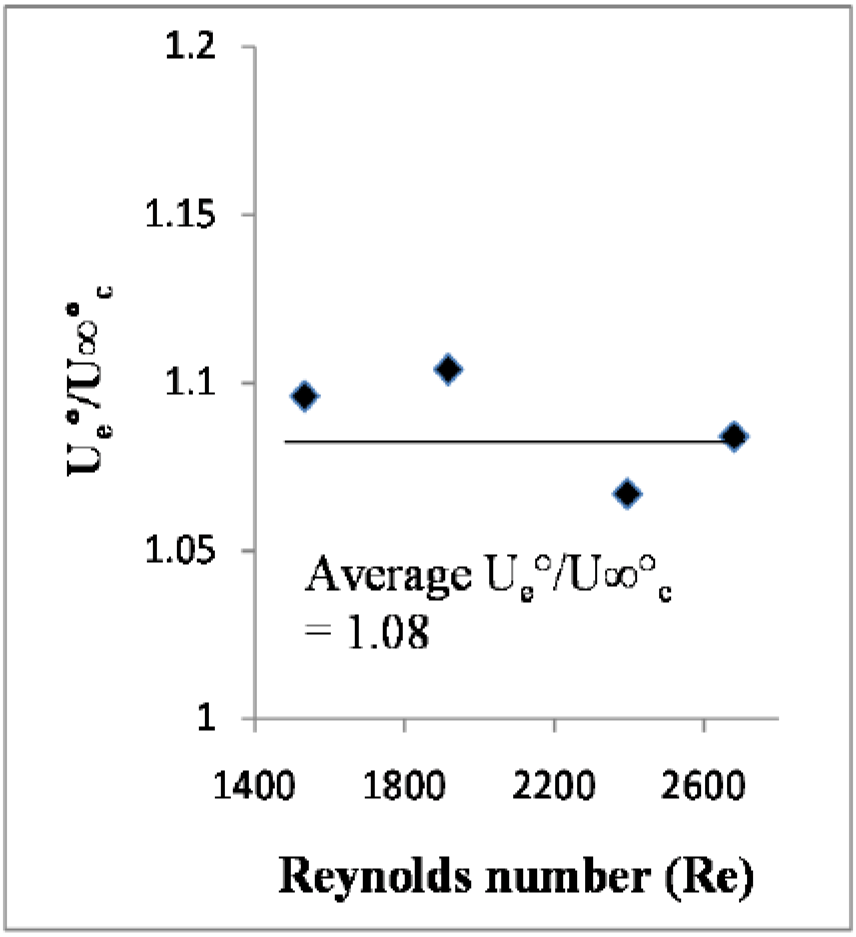

Fig.18. Water velocity near the edge of the disk normalized to its value in the upstream of the disk corrected according to the new flow area $U∞°_c$ measured using hydrogen bubble technique versus Reynolds number